

Phase Diagram and Thermodynamic Properties of the Square Lattice of Antiferromagnetic Spin-1/2 Triangles in $\text{La}_4\text{Cu}_3\text{MoO}_{12}$

Stefan Wessel and Stephan Haas

Department of Physics and Astronomy, University of Southern California, Los Angeles, CA 90089-0484
(November 5, 2018)

The magnetic phase diagram and the thermodynamic properties of a square lattice containing antiferromagnetically coupled spin-1/2 triangles are studied. A Heisenberg Hamiltonian with three strong intra-triangle exchange coupling constants and one weak inter-triangle exchange coupling constant is proposed to model the interacting Cu^{2+} ions of the Cu_3MoO_4 planes in $\text{La}_4\text{Cu}_3\text{MoO}_{12}$. Depending on the ratio of the intra-triangle coupling constants, various long-ranged magnetic phases are shown to compete at low temperatures. A comparison of numerical calculations of thermodynamic properties in the model Hamiltonian with recent experiments on $\text{La}_4\text{Cu}_3\text{MoO}_{12}$ suggests that the spins in this material order antiferromagnetically along the x-direction and ferromagnetically along the y-direction of the Cu_3MoO_4 planes. The temperature dependence of the uniform magnetic susceptibility, the heat capacity, and the entropy are calculated and are shown to be in qualitative agreement with the experiments on this compound.

It is known that the zero-point fluctuations in two-dimensional (2D) quantum antiferromagnets are responsible for a strong renormalization of their order parameter, causing a substantial correction of the sublattice magnetization in long-ranged antiferromagnets such as La_2CuO_4 ¹, or completely suppressing the magnetic moment in short-range-ordered antiferromagnetic (AF) compounds such as the structurally frustrated Kagome lattice, containing coupled spin-1/2 triangles.²⁻⁴ In contrast to systems with long-range AF order, this spin liquid is best described within a resonant valence bond picture that accounts for the degeneracy of the ground state, the singlet-triplet spin gap, and the large number of low-lying singlet states in the thermodynamic limit²⁻⁴.

Recently, thermodynamic measurements on the triangular cluster compound $\text{La}_4\text{Cu}_3\text{MoO}_{12}$ were reported⁵. This system is a layered material, containing planar Cu_3MoO_4 square lattices of nearly isosceles Cu^{2+} spin-1/2 triangles, as shown in Fig. 1. In contrast to the Kagome antiferromagnet, $\text{La}_4\text{Cu}_3\text{MoO}_{12}$ orders antiferromagnetically at a Néel temperature of 2.6K despite the structural frustration within the triangles. This indicates that - unlike the Kagome lattice - the bipartite nature of the square lattice of triangles in this compound is essential for the long-range ordering. Associated with the antiferromagnetic ordering transition, an entropy change of 1.56 J/(K mol Cu) was observed. Furthermore, a plateau in the magnetization above a critical field of approximately 20 T was reported.

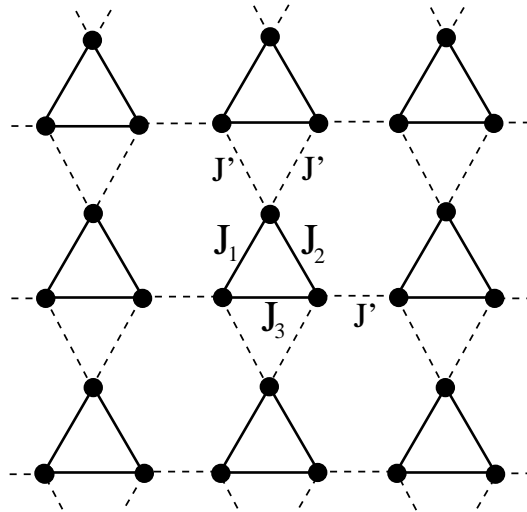


FIG. 1. Square lattice of Cu^{2+} triangles in the Cu_3MoO_4 planes of $\text{La}_4\text{Cu}_3\text{MoO}_{12}$. The intra-triangle couplings J_1 , J_2 , and J_3 are strong compared to the inter-triangle couplings J' .

From the different Cu-O bond lengths within and between the triangles,⁵ it can be concluded that the intra-

triangle couplings J_1 , J_2 , and J_3 are much stronger than the inter-triangle coupling J' . The magnetic moments of the neighboring Cu^{2+} ions within the Cu_3MoO_4 planes interact via antiferromagnetic superexchange, mediated by the filled O^{2-} p-orbitals. This leads us to propose a planar model Hamiltonian of weakly coupled spin-1/2 trimers for $\text{La}_4\text{Cu}_3\text{MoO}_{12}$, given by

$$H = \sum_{\mathbf{r}} [J_1 \mathbf{S}_{\mathbf{r},1} \cdot \mathbf{S}_{\mathbf{r},2} + J_2 \mathbf{S}_{\mathbf{r},2} \cdot \mathbf{S}_{\mathbf{r},3} + J_3 \mathbf{S}_{\mathbf{r},3} \cdot \mathbf{S}_{\mathbf{r},1} + J'(\mathbf{S}_{\mathbf{r},3} \cdot \mathbf{S}_{\mathbf{r}+\mathbf{x},1} + \mathbf{S}_{\mathbf{r},2} \cdot \mathbf{S}_{\mathbf{r}+\mathbf{y},1} + \mathbf{S}_{\mathbf{r},2} \cdot \mathbf{S}_{\mathbf{r}+\mathbf{y},3})], \quad (1)$$

where $\mathbf{S}_{\mathbf{r},j}$ represents a spin-1/2 degree of freedom at site j of the triangle centered at position \mathbf{r} . The underlying 2D square lattice of triangles is spanned by the unit vectors \mathbf{x} and \mathbf{y} . In order to account for deviations from perfect isosceles triangles, 3 different intra-triangle couplings are considered. From experience, it is rather difficult to derive the precise exchange constants from first principles.⁶ An alternative approach is to determine them by comparing results of model calculations on H to experimental data. However, this approach is typically complicated by the fact that various parameter sets may fit the experimental results equally well.⁷ In the following, we will therefore first examine the weak-coupling phase diagram of H . Subsequently, the recent experiments on $\text{La}_4\text{Cu}_3\text{MoO}_{12}$ will be analyzed, based on numerical calculations for the proposed model Hamiltonian in the relevant parameter regime.

The weak-coupling ($J' \ll J_1, J_2, J_3$) zero-temperature phase diagram of H is determined by the dominant spin-spin correlation function of the total trimer spins $\bar{\mathbf{S}}_{\mathbf{r}} = \mathbf{S}_{\mathbf{r},1} + \mathbf{S}_{\mathbf{r},2} + \mathbf{S}_{\mathbf{r},3}$, defined by $S_{\mathbf{q}} = \sum_{\mathbf{r}} \exp(i\mathbf{q} \cdot \mathbf{r}) \langle \bar{\mathbf{S}}_{\mathbf{0}} \cdot \bar{\mathbf{S}}_{\mathbf{r}} \rangle$. We have calculated this quantity by exact numerical diagonalization of finite clusters with periodic boundary conditions for small inter-triangle coupling strengths J' .⁸ It is found that the wave vector of the dominant spin-spin correlation function strongly depends on the relative strengths of the intra-triangle couplings J_1 , J_2 , and J_3 . The resulting zero-temperature phase diagrams for square lattices of weakly coupled triangles are shown in Fig. 2 with (a) $J' = 0.01J_3$, and (b) $J' = 0.1J_3$, where the various phases are labeled by their magnetic ordering wave vectors $\mathbf{Q} = (q_x, q_y)$.

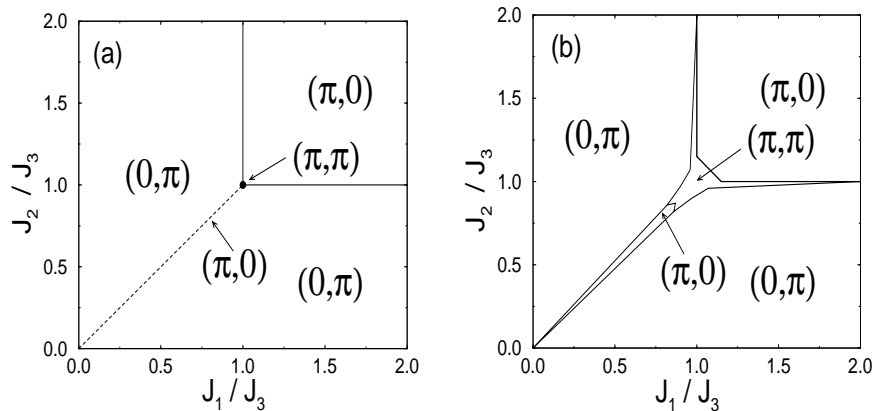


FIG. 2. Zero-temperature magnetic phase diagram of the AF spin-1/2 trimer square lattice with a weak inter-triangle coupling (a) $J' = 0.01J_3$ and (b) $J' = 0.1J_3$.

Since the model Hamiltonian H is invariant under $J_1 \leftrightarrow J_2$, these phase diagrams have reflection symmetry about the diagonal axis $J_1 = J_2$. All exchange coupling constants have been scaled by the intra-triangle coupling constant along the x-direction, J_3 . In Fig 2(a), the phase diagram is shown for the ultra-weak-coupling limit with a small inter-triangle coupling $J' = 0.01J_3$. At the isotropic point $J_1 = J_2 = J_3$, the system orders antiferromagnetically in both planar directions, resulting in an ordering wave vector $\mathbf{Q} = (\pi, \pi)$. For small J_3 ($J_3 < J_1, J_2$), the system decouples into spin-1/2 AF chains along the x-direction with weak residual ferromagnetic (FM) couplings along the y-direction, leading to $\mathbf{Q} = (\pi, 0)$. In contrast, in the regimes $J_1 \gg J_2, J_3$ and $J_2 \gg J_1, J_3$, the model describes effective spin-1/2 AF chains along the y-axis with weak residual FM coupling along the x-direction, and thus $\mathbf{Q} = (0, \pi)$. The symmetry line $J_1 = J_2$ with $\mathbf{Q} = (\pi, 0)$ is found to separate these two $\mathbf{Q} = (0, \pi)$ phases.⁹

As the inter-triangle coupling J' is increased (Fig. 2(b)), a finite region with $\mathbf{Q} = (\pi, \pi)$ opens up, centered around the isotropic point $J_1 = J_2 = J_3$. Furthermore, the $\mathbf{Q} = (\pi, 0)$ regime is found to extend away from the diagonal $J_1 = J_2$ line. It has been proposed that the AF ordered low-temperature phase of $\text{La}_4\text{Cu}_3\text{MoO}_{12}$ may fall into the $\mathbf{Q} = (\pi, \pi)$ regime.⁵ However, as we will discuss in the following, a numerical analysis of the thermodynamic properties of H - in particular the magnetic entropy - suggests that this compound should be placed in the regime of weak J_3 with $\mathbf{Q} = (\pi, 0)$ rather than in the $\mathbf{Q} = (\pi, \pi)$ regime close to the isotropic point.

When analyzing the thermodynamic response functions for the square lattice of weakly coupled AF spin-1/2 triangles, three temperature regimes can be identified. At high temperatures $T > J_1, J_2, J_3$, the system is a paramagnetic

ensemble of thermally decoupled spins. Upon lowering the temperature into the region $J' < T < J_1, J_2, J_3$, the intra-triangle couplings become relevant, and spin doublets are formed on each triangle. The properties of the system in this temperature interval are thus well characterized by a thermodynamic ensemble of decoupled trimers with effective spin-1/2 degrees of freedom. Below the ordering transition temperature $T_N \approx J'$ the small inter-triangle couplings correlate these spin-1/2 trimers, leading to long-range-ordered magnetic phases with characteristic \mathbf{Q} vectors that depend on the ratio of the intra-triangle coupling constants, as discussed above. We have determined the temperature dependence of the uniform magnetic susceptibility, the heat capacity, and the entropy from full numerical diagonalizations of H on finite clusters with periodic boundary conditions. Results representative for the the $\mathbf{Q} = (\pi, 0)$ phase with $(J_1, J_2, J_3) = (1.5, 1.5, 1.0)$, $\mathbf{Q} = (0, \pi)$ phase with $(J_1, J_2, J_3) = (0.5, 1.0, 1.0)$, and the $\mathbf{Q} = (\pi, \pi)$ phase with $(J_1, J_2, J_3) = (1.0, 1.0, 1.0)$ are shown in Fig. 3.

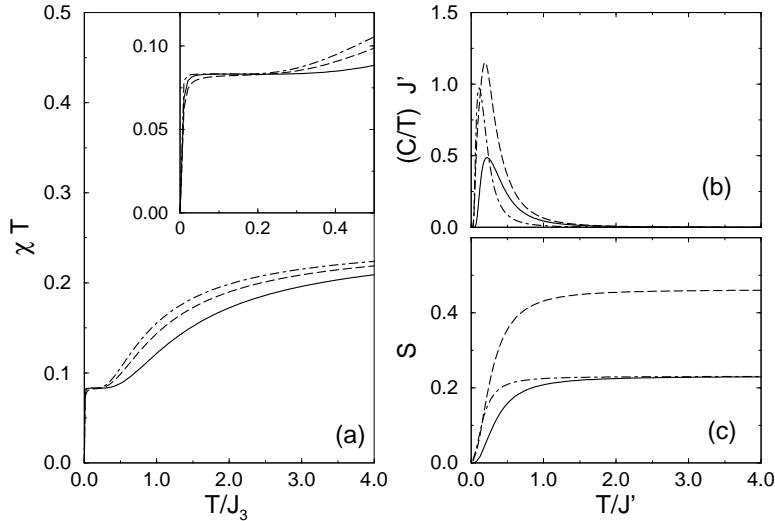


FIG. 3. Thermodynamic response in the square lattice of AF spin-1/2 triangles. (a) Temperature-dependent uniform susceptibility in the $\mathbf{Q} = (\pi, 0)$ regime (solid line), the $\mathbf{Q} = (0, \pi)$ regime (dot-dashed line), and the $\mathbf{Q} = (\pi, \pi)$ regime (dashed line). The inset shows the intermediate-temperature plateaus of χT at $\frac{1}{12}$. (b) Temperature dependence of the specific heat, and (c) the magnetic entropy per site.

The three distinct temperature regimes are clearly observed in the uniform susceptibilities, shown in Fig. 3(a). At high temperatures the spins are effectively uncorrelated with a Curie constant $\lim_{T \rightarrow \infty} [\chi T] = C = \frac{1}{4}$. At intermediate temperatures there is a plateau in χT with a reduced effective Curie constant $C' = \frac{1}{12}$, associated with the paramagnetic response of uncorrelated spin-1/2 trimers, containing three spins each. Finally, at low temperatures of order J' these trimers condense into magnetically ordered phases, leading to an additional reduction in χT . These trends in the temperature dependence of the uniform susceptibilities are similar in all three parameter regimes. Furthermore, the shape of $\chi(T)$ is found to be in good qualitative agreement with measurements on $\text{La}_4\text{Cu}_3\text{MoO}_{12}$ (see Fig. 2 of Ref.⁵), which show an onset of magnetic ordering at 2.6 K, two orders of magnitude smaller than the observed threshold temperature for trimer formation at approximately 250 K.

In Figs. 3 (b) and (c) the specific heat and the magnetic entropy per site are shown. The onset of the intermediate regime in which intra-triangle correlations become relevant is marked by the maxima in the specific heat divided by the temperature, C/T , consistent with the onsets of the plateaus in χT , seen in Fig. 3(a). For the $\mathbf{Q} = (\pi, 0)$ and the $\mathbf{Q} = (0, \pi)$ regimes, the entropies per site exhibit plateaus at $S = \frac{1}{3} \ln 2$, rising up to $\ln 2$ at high temperatures (not shown in the figure). Hence, only 1/3 of the magnetic entropy is released in the intermediate temperature regime, corresponding to an ensemble of $N/3$ trimer doublets with a decreased paramagnetic moment of spin-1/2 per trimer. In contrast, the entropy for the isotropic coupling case with $\mathbf{Q} = (\pi, \pi)$ shows a larger plateau value of $\frac{1}{3} \ln 4$, associated with the degeneracy of two Kramers doublets in this regime. In fact, the same plateau value is found over the whole $\mathbf{Q} = (\pi, \pi)$ regime centered around the isotropic coupling point. At very high temperatures the entropy saturates at the fully paramagnetic value of $\ln 2$ in all cases. A comparison with the experiments on $\text{La}_4\text{Cu}_3\text{MoO}_{12}$ (Fig. 3 in Ref.⁵) clearly favors the smaller intermediate-temperature plateau value of $\frac{1}{3} \ln 2$ over $\frac{1}{3} \ln 4$, suggesting that the low-temperature magnetic order in this material is characterized by $\mathbf{Q} = (\pi, 0)$ or $\mathbf{Q} = (0, \pi)$ rather than by $\mathbf{Q} = (\pi, \pi)$.

Examining the intra-triangle bond lengths and bond angles in the Cu_3MoO_4 planes of $\text{La}_4\text{Cu}_3\text{MoO}_{12}$ (table 1 of

Ref.⁵), it appears likely that J_3 is smaller than both J_1 and J_2 .^{6,10} This suggests that the magnetically ordered low-temperature phase in this compound is part of the $\mathbf{Q} = (\pi, 0)$ regime rather than the $\mathbf{Q} = (0, \pi)$ regime. Neutron scattering studies should help to verify this conjecture.

In summary, we have studied the magnetic phase diagram and the thermodynamic response of a square lattice containing weakly coupled AF spin-1/2 triangles. A Heisenberg Hamiltonian with three strong intra-triangle exchange coupling constants and a weak inter-triangle exchange coupling constant is proposed to model the interacting Cu^{2+} ions of the Cu_3MoO_4 planes in $\text{La}_4\text{Cu}_3\text{MoO}_{12}$. Depending on the ratio of the intra-triangle coupling constants, various long-ranged magnetic phases are possible at low temperatures. A comparison of numerical calculations of the thermodynamic properties in the proposed model Hamiltonian with recent experiments on $\text{La}_4\text{Cu}_3\text{MoO}_{12}$ leads us to suggest that the magnetically ordered phase in this compound belongs to the $\mathbf{Q} = (\pi, 0)$ regime rather than the $\mathbf{Q} = (0, \pi)$ or the $\mathbf{Q} = (\pi, \pi)$ regimes of the model. The ordering wave vector could be determined in a neutron scattering study, giving conclusive information regarding the nature of the magnetically ordered phase in this material.

We wish to thank M. Azuma, A. Honecker, B. Normand, and M. Takano for useful discussions. The hospitality of the Los Alamos National Laboratory and the financial support of the Zumberge foundation are acknowledged.

¹ E. Manousakis, Rev. Mod. Phys., Vol. 63, No. 1, 1 (1991) and references therein.

² P. Lecheminant, B. Bernu, C. Lhuillier, L. Pierre, and P. Sindzingre, Phys. Rev. B **56**, 2521 (1997).

³ F. Mila, Phys. Rev. Lett. **81**, 2356 (1998).

⁴ P. Sindzingre, G. Misguich, C. Lhuillier, B. Bernu, L. Pierre, C. Waldtmann, and H.-U. Everts, Phys. Rev. Lett. **84**, 2953 (2000).

⁵ M. Azuma, T. Odaka, M. Takano, D. A. Vander Griend, K. R. Poeppelmeier, Y. Narumi, K. Kindo, Y. Mizuno and S. Maekawa, Phys. Rev. B **62**, R3588 (2000).

⁶ D. Bloch, J. Phys. Chem. Solids **27**, 881 (1966).

⁷ An illustrative example for this point is the recent controversy on the correct set of exchange parameters for CuGeO_3 . See e.g. T. Barnes and J. Riera, Phys. Rev. B **50**, 6817 (1994) and G. Castilla, S. Chakravarty, and V.J. Emery, Phys. Rev. Lett. **75**, 1823 (1995).

⁸ We have studied lattices with 6, 12, and 18 spins.

⁹ The phase diagram in Fig. 2(a) is confirmed by lowest-order perturbation theory in the weak inter-triangle coupling J' . In this limit, the model Hamiltonian can be mapped onto a square lattice of spin-1/2 degrees of freedom with effective anisotropic exchange coupling constants along the x- and y-directions. For example in the limit of small J_3 with $J_1 = J_2 > J_3$ this procedure leads to an effective Heisenberg Hamiltonian with antiferromagnetic exchange couplings along the x-direction and ferromagnetic exchange couplings along the y-direction, $H_{eff}^{(\pi,0)} = \sum_r \left[\frac{4}{9} J' \tilde{\mathbf{S}}_r \cdot \tilde{\mathbf{S}}_{r+x} - \frac{4}{9} J' \tilde{\mathbf{S}}_r \cdot \tilde{\mathbf{S}}_{r+y} + \frac{1}{4} J_3 - J_1 \right]$. Similarly, along the line $J_3 = J_2 > J_1$, one finds $H_{eff}^{(0,\pi)} = \sum_r \left[-\frac{2}{9} J' \tilde{\mathbf{S}}_r \cdot \tilde{\mathbf{S}}_{r+x} + \frac{2}{9} J' \tilde{\mathbf{S}}_r \cdot \tilde{\mathbf{S}}_{r+y} - \frac{1}{2} J_3 - \frac{1}{4} J_1 \right]$.

¹⁰ Using $J_i \propto 1/d_i^\alpha$, with $\alpha > 1$ and d_i the interatomic distance along the bond J_i , $J_3 < J_1 \approx J_2$ follows from $d_3 > d_1 \approx d_2$.^[5]